

Minority Carrier Annihilation in Lateral Direction Caused by Recombination Defects at Cut Edges and Bare Surfaces of Crystalline Silicon

Toshiyuki Sameshima*, Jun Furukawa, and Shinya Yoshidomi

Tokyo University of Agriculture and Technology, Koganei, Tokyo 184-8588, Japan

E-mail: tsamesim@cc.tuat.ac.jp

Received August 4, 2012; accepted January 12, 2013; published online March 19, 2013

We report on the photo-induced minority carrier annihilation effect in the lateral direction caused by cut edges and partially formed bare surfaces for 500- μm -thick n-type silicon substrates coated with thermally grown SiO_2 layers. A 9.35 GHz microwave transmittance measurement system with illumination with a 0.2-cm-wide 635-nm continuous wave light beam was used to measure spatial distribution of the minority carrier effective lifetime τ_{eff} . A mechanical cut decreased τ_{eff} in a 0.9-cm-wide region from the cut edges. τ_{eff} decreased from 3.4×10^{-3} (initial) to 6.5×10^{-4} s at cut edges. A simple model of carrier diffusion in the lateral direction with a carrier lifetime of 3.4×10^{-3} s and a recombination velocity of 500 cm/s at the cut edges well explained the experimental spatial change in τ_{eff} near the cut edges. A similar widely spatial decrease in τ_{eff} was also observed in the region coated with thermally grown SiO_2 layers near the bare silicon surface formed by partial etching of SiO_2 .

© 2013 The Japan Society of Applied Physics

1. Introduction

Minority carriers are essential for semiconductor devices such as photosensors and solar cells.¹⁻³⁾ A high minority carrier lifetime and low density of carrier recombination defect states are required for achieving high-performance photosensors and solar cells. Carrier recombination defect states seriously affect the minority carrier effective lifetime of silicon because crystalline silicon generally has a long bulk lifetime and a large diffusion length owing to the indirect band gap. Excellent techniques and models for analyzing minority carrier lifetime and carrier recombination defect states have been reported.⁴⁻¹²⁾ We have also developed techniques for measuring the density of minority carriers and the minority carrier effective lifetime τ_{eff} using a 9.35 GHz microwave transmittance measurement system with continuous wave (CW) as well as periodic pulsed light illumination.¹³⁻¹⁵⁾ We have established the relationship of the density of minority carriers with τ_{eff} in cases of CW and periodic pulsed light illumination. Investigation of minority carrier behavior under CW light illumination is important for development of solar cells because of their usage under CW sunlight.

Spatial analysis of carrier recombination is also important for producing large devices with a high quality. A high density of localized carrier recombination defect states causes spatial changes in τ_{eff} around the defects. For example, mechanical and laser cutting have been widely used for production of various silicon devices including photosensors and solar cells.^{16,17)} But they can generate carrier recombination states at the cut edges. The cutting process inevitably leads to a silicon bare surface. Although a cut cross-sectional area is very limited in space because of thin substrates, a silicon bare surface can have a high density of carrier recombination sites. Several important investigations by microwave-photoconductance decay, quasi-steady state photoconductance and photoluminescence methods have been reported.¹⁸⁻²⁰⁾ The recombination velocity and carrier diffusion are important factors for analyzing spatial changes in τ_{eff} .

In this paper, we report on the precise investigation of spatial changes in τ_{eff} caused by localized carrier recombi-

nation defect states. For localized carrier recombination defect states, we concentrate the cut edges and partially formed a bare surface for n-type silicon substrates coated with thermally grown SiO_2 layers. We fabricated a light beam irradiation device with an optical slit in our microwave transmittance equipment to measure the spatial changes in τ_{eff} . We report that τ_{eff} and minority carrier density decrease in a wide region from the cut edges. By numerical analysis of carrier generation and diffusion in the lateral direction and annihilation at the cut edges, we show that the carrier recombination effect at the cut edges is not negligible. We also report the decrease in τ_{eff} in the region coated with thermally grown SiO_2 in the lateral direction toward the region partially formed with bare silicon surface. τ_{eff} markedly decreased to a low values in regions close to the bare silicon edges.

2. Experimental Procedure

Three 20 Ωcm n-type silicon substrates with an orientation of (100) and a thickness of 500 μm formed by the Czochralski (CZ) process were prepared. The top and rear surfaces were coated with 100-nm-thick thermally grown SiO_2 layers formed in dry oxygen atmosphere at 1100 $^\circ\text{C}$. An one substrate was mechanically cut in the middle region into two half-moon-shaped pieces in air atmosphere at room temperature. After keeping the sample pieces in air atmosphere at room temperature for two days, transparent vinyl tapes were used to join the two cut pieces with a gap less than 100 μm , as shown by a schematic cross section of a sample, as shown in Fig. 1(a). The second substrate coated with 100-nm-thick SiO_2 was cut with a size of 2.3×1.0 cm^2 . The sample was also kept in air atmosphere at room temperature for two days. For the third substrate, the SiO_2 layer in the left half region was removed at the top and rear surfaces using diluted hydrofluoric acid, as shown in Fig. 1(b). it was also kept in air atmosphere for two days.

We used a 9.35 GHz microwave transmittance measurement system with waveguide tubes, which had a narrow gap for placing a sample wafer, as shown in Fig. 2(a).^{13,14)} The X-Y moving stage moved the sample to measure τ_{eff} spatial distribution. A 635 nm CW laser diode light was introduced into the waveguide tube, as shown in Fig. 2(b). The light

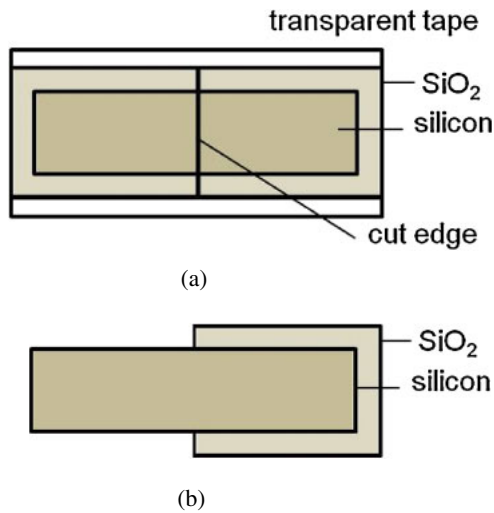


Fig. 1. (Color online) Schematic images of cross section of silicon samples cut in the middle region (a), and coated with SiO₂ in the right half and bare surface in the left surface (b).

intensity was set at 1.5 mW/cm² at the sample surface. The light illumination induced free carrier generation in the top 3-μm-surface region.²¹⁾ The microwave, which transmitted samples, was rectified using a high-speed diode and was integrated. The integrated voltage was detected by a digital electrometer and analyzed to precisely obtain the carrier density per unit area *N*. *N* has a proportional relation to

τ_{eff} with a parameter of the carrier generation rate per unit area *G* follows as,^{13,14,22)}

$$N = G \times \tau_{\text{eff}}, \quad (1)$$

Because of uncertainties of quantum efficiency and light reflection loss in *G*, we calibrated τ_{eff} for the initial sample coated with thermally grown SiO₂ layers by measurement of 50% duty periodically pulsed light illumination method with 635 nm light, which gave τ_{eff} independent of *G*.¹⁴⁾ To avoid change in τ_{eff} with photon flux,²⁰⁾ we used the same average light intensity for the periodic pulsed light illumination method as that of CW light.

For the present purpose, a 0.2-cm-wide light beam was formed by black sheets slit attached at the surface of the waveguide tube, as shown in Fig. 2(b).²³⁾ The black sheet completely shaded 635 nm light, while they are transparent to the 9.35 GHz microwave. The sample cut into the two half moon shapes shown in Fig. 1(a) was placed facing to the surface of the waveguide tube. The τ_{eff} spatial distribution in the *X*-direction was measured as a function of the central position of the light beam *X*₁. The sample was moved by a stage, as shown in Fig. 2(b). When the center of the light beam illuminates to the cut edge, *X*₁ is 0 cm. The detection limit of τ_{eff} in the present light beam under the low-light-intensity condition was about 1 × 10⁻⁶ s. The τ_{eff} spatial distribution in the *X*-direction was also measured for the initial 4-in. samples prior to making cut edges for comparison. Then, we removed the black sheet slit from the waveguide tube to illuminate the sample entirely in the

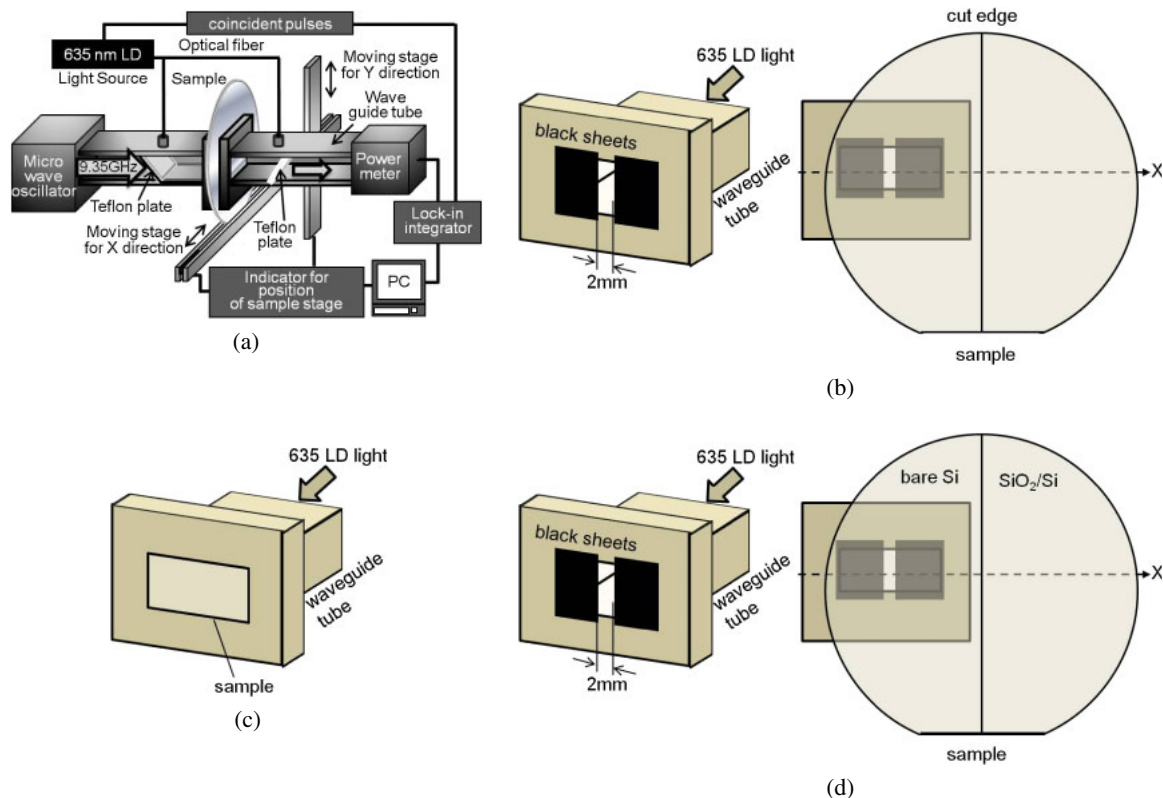


Fig. 2. (Color online) Schematic of apparatus for measuring τ_{eff} by photo-induced carrier microwave absorption (a), image of experimental measurement of τ_{eff} spatial distribution across the cut edge (b), image of experimental measurement of τ_{eff} for sample with the same size as the cross-sectional area of the waveguide tube (c), and image of experimental measurement of τ_{eff} spatial distribution in the region coated with thermally grown SiO₂ layers and bare surface (d).

waveguide tube. τ_{eff} was measured for the sample coated with 100-nm-thick SiO₂ cut into a size of $2.3 \times 1.0 \text{ cm}^2$, which was the same size as that of the cross sectional area of the waveguide tube, as shown in Fig. 2(c) to demonstrate the cut edge effect on τ_{eff} . Prior to cutting samples, τ_{eff} was also measured at the same position of the cut area for the initial 4-in. sample for comparison.

The black sheet slit was attached again to form a 0.2-cm-wide light beam. The τ_{eff} spatial distribution in the X -direction was measured for the sample with SiO₂ remaining in the right half and the bare surface in the left half, as shown in Fig. 2(d). The τ_{eff} spatial distribution in the X -direction was also measured for the initial 4-in. samples prior to removal of SiO₂ in the left region for comparison.

3. Results and Discussion

Figure 3 shows the τ_{eff} spatial distributions for the n-type sample with the cut edges as a function of X_1 from -2.0 to 2.0 cm. In this measurement region, the light beam was always kept 3 cm at least far from the circular wafer edges. The initial sample had τ_{eff} in the range from 2.9×10^{-3} to 3.6×10^{-3} s. It means that the silicon surfaces were passivated well with the thermally grown SiO₂ layers. If the experimental τ_{eff} is governed by the surface recombination velocity S for both surfaces, experimental τ_{eff} gave S in the range from 6.9 to 8.6 cm/s. The almost the same distribution of τ_{eff} was observed for X_1 larger than 0.9 cm or smaller than -0.9 cm for the sample with the cut edges. τ_{eff} gradually decreased when X_1 approached to the cut edge. τ_{eff} finally decreased to 6.5×10^{-4} s at 0 cm, as shown in Fig. 3. This means that substantial carrier annihilation occurred when light was illuminated at the cut edges. This result clearly shows that the 0.9-cm-wide region suffered from the carrier recombination effect at the cut edges. Clean surfaces would be formed immediately after cleavage of (100) silicon substrates. Small atomic steps were probably formed periodically according to the crystalline lattice.²⁴ It probably resulted in a rather stable superstructure on the cleaved surfaces. However, the oxygen atoms came to the surface from the air immediately after the sample was cut. Si-O bonding formation changed the structural and electronic states²⁵ when the samples was kept in air atmosphere. Substantial surface states causing carrier recombination were probably formed.

In order to investigate the physics of the decrease in τ_{eff} shown in Fig. 3, the numerical analysis program of carrier diffusion and annihilation using the finite differential element method were constructed as our previous study.¹³ Under the present experimental conditions, the light beam with a 0.2 cm width in the lateral X -direction and a 1.0 cm length in the vertical direction was illuminated in the waveguide tube, as shown in Fig. 2(b). Therefore, in the region of the sample, which the microwave transmitted in the waveguide tube, photo-induced carriers were assumed to diffuse in the lateral X -directions with τ_{eff} and the diffusion coefficient D from the point of light illumination with a light beam width of L , and carrier generation rate g per unit volume. The carrier lifetime was used as the experimental τ_{eff} of 3.4×10^{-3} s measured at 0 cm in advance of sample cutting under the assumption of a successfully high enough carrier diffusion in the depth direction. The carriers were annih-

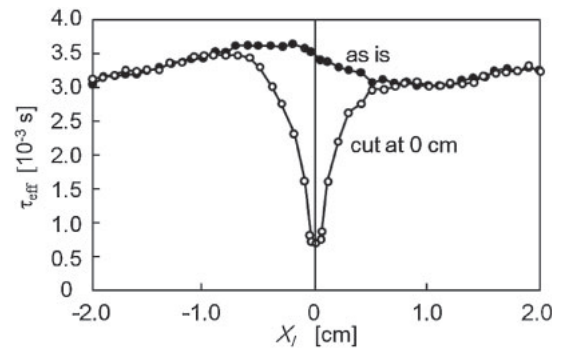


Fig. 3. Spatial distributions of τ_{eff} as a function of X_1 with the cut position at 0 cm. Solid and open circles present data for the initial sample and the sample cut at the middle region, respectively.

lated at the cut edges with a recombination velocity S_E . The photo-induced carrier density per unit volume $N_{\text{photo}}(X)$ is given using the carrier diffusion model under a steady-state condition as^{13,22}

$$D \frac{d^2 N_{\text{photo}}(X)}{dX^2} - \frac{N_{\text{photo}}(X)}{\tau_{\text{eff}}} + g(X) = 0, \quad (2)$$

where $g(X)$ is the carrier generation rate, which depends on X . The $g(X)$ is a constant value of g at the position in the range from $X_1 - L/2$ to $X_1 + L/2$. The total carrier generation rate is $g \times L$ ($= G$) when X_1 is larger than or equal to $L/2$. On the other hand, it is $g \times (L/2 + X_1)$ when light illuminates in the region near the sample edge and X_1 was lower than $L/2$. We additionally placed the boundary condition of carrier annihilation with S_E at the cut edges. When X_1 is larger than $L/2$, no light illuminates at the edges. The boundary condition is given as^{13,22}

$$D \frac{dN_{\text{photo}}}{dX} \Big|_{X=0} = S_E N_{\text{photo}}(0), \quad X_1 > \frac{L}{2}, \quad (3)$$

On the other hand, when X_1 is lower than $L/2$, the edge region is illuminated by light. The boundary condition is given as

$$D \frac{dN_{\text{photo}}}{dX} \Big|_{X=0} = S_E N_{\text{photo}}(0) - g \Delta X, \quad X_1 \leq \frac{L}{2}, \quad (4)$$

where ΔX is the unit lattice distance for calculation of finite elements.

Figure 4 shows the experimental ratio of τ_{eff} of the initial sample to that of the cut sample, and calculated arbitrary τ_{eff} with D of $12 \text{ cm}^2/\text{s}$ and different S_E values of 0, 50, 100, 200, 300, 500, 1000, and 5000 cm/s as functions of X_1 from the cut edge from 0 to 1.0 cm. D was obtained from the Einstein formula $D = \mu kT/e$, where k is the Boltzmann constant, T is an absolute temperature of 300 K at room temperature, e is the elemental charge of 1.6×10^{-19} C, and μ is a hole mobility of $470 \text{ cm}^2 \text{ V}^{-1} \text{ s}^{-1}$ at a donor density of $2 \times 10^{14} \text{ cm}^{-3}$ given by a resistivity of $20 \text{ } \Omega \text{ cm}$.²⁶ The experimental ratio of τ_{eff} gradually decreased from 1.0 to 0.2 as X_1 decreased from 0.9 to 0 cm. The calculated ratio of τ_{eff} was 1.0 in the range of X_1 values from 1.0 to 0.1 cm, while it linearly decreased to 0.5 in the range of X_1 values from 0.1 to 0 cm in the case of a S_E of 0 cm/s. Zero S_E caused no carrier recombination, while the calculated ratio

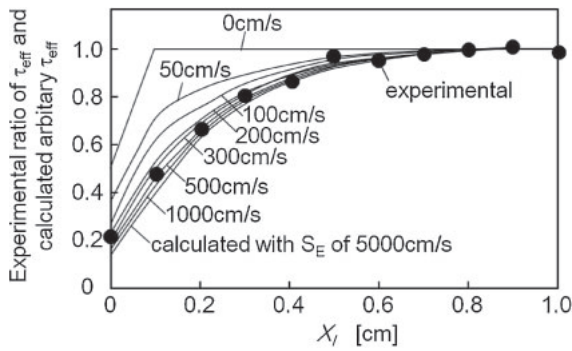


Fig. 4. Experimental ratio of τ_{eff} of the initial sample to that of cut sample, and calculated arbitrary τ_{eff} with D of $12 \text{ cm}^2/\text{s}$ and different S_E values of 300, 500, 1000, and 5000 cm/s as functions of X_1 from the cut edge from 0 to 1.0 cm.

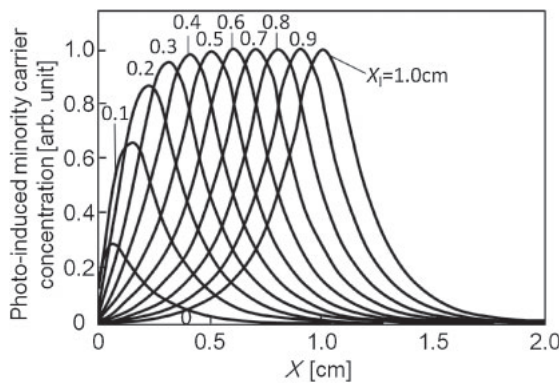


Fig. 5. Arbitrary calculated photo-induced lateral distribution of hole minority carrier concentration at different positions of light illumination X_1 between 0 and 1.0 cm from the cut edge with the S_E of 500 cm/s .

of τ_{eff} decreased because the total carrier generation rate decreased near the cut edges. In the case of S_E higher than zero, the calculated ratio of τ_{eff} gradually decreased as X_1 decreased from 0.9 to 0 cm because of the carrier recombination effect. The experimental ratio of τ_{eff} was well traced by calculated curves with S_E in the range from 300 to 5000 cm/s . This shows that the decrease in experimental τ_{eff} resulted from the decrease in the photo-induced hole minority carrier density owing to carrier annihilation by S_E at the cut edges. However, the calculated ratio of τ_{eff} had similar curves for S_E values from 300 to 5000 cm/s . This is because the low D limited carrier diffusion over a long distance, especially longer than the carrier diffusion length $[(D \cdot \tau_{\text{eff}})^{0.5} \sim 0.2 \text{ cm}]$ from the cut edges. It is therefore difficult to determine S_E from the analysis shown in Fig. 4. Although the most possible S_E was given as 500 cm/s , 5000 cm/s would also be possible given in the present accuracy. Figure 5 shows that arbitrary calculated photo-induced lateral distribution of hole minority carrier concentration with different X_1 values between 0 and 1.0 cm from the cut edges with the S_E of 500 cm/s . Continuous carrier generation induced by light illumination with the 0.2 cm beam width gave a broad and symmetrical shape of hole carriers when X_1 values were 0.9 and 1.0 cm, that is, far from the cut edges. Although the light beam width was 0.2 cm, the carrier density widely distributed with a full

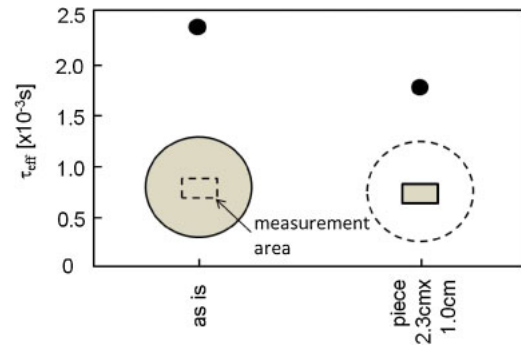


Fig. 6. (Color online) τ_{eff} measured in the middle region for 4-in. n-type whole silicon substrate samples coated with thermally grown SiO_2 layers and τ_{eff} measured in the same area for the silicon sample cut with the same size as that of the cross section of the waveguide tube.

width at e^{-1} maximum of 0.6 cm because of carrier annihilation with the τ_{eff} of $3.4 \times 10^{-3} \text{ s}$. The S_E at the edges was not important for the cases of X_1 values of 0.9 and 1.0 cm. On the other hand, the peak concentration decreased and the shape of the carrier density became asymmetric as X_1 approached to the cut edges. Minority carrier concentration steeply decreased to 0 as X decreased to 0 cm because of the carrier annihilation due to S_E .

Although the experimental result of decrease in τ_{eff} shown in Fig. 3 was well explained by the simple model of carrier diffusion in the lateral direction and annihilation by the recombination defect states at the cut edges, as shown in Figs. 4 and 5, we could not deny the possibility that carrier recombination defects might be formed inside a region deep enough to cause a decrease in τ_{eff} in a region far from the cut edge because mechanical cutting was a very radical process.

Figure 6 shows the changes in τ_{eff} for samples with a size of $2.3 \times 1.0 \text{ cm}^2$, which was the same size as that of the cross section of the waveguide tube, as shown in Fig. 2(d). τ_{eff} was high of $2.4 \times 10^{-3} \text{ s}$, in the middle region of the whole 4-in. substrate coated with thermally grown SiO_2 layers in advance of cutting. On the other hand, the sample cut with the size of $2.3 \times 1.0 \text{ cm}^2$ had a low τ_{eff} of $1.7 \times 10^{-3} \text{ s}$. Although the silicon piece completely covered the waveguide tube, τ_{eff} decreased by 30% of the initial value owing to the carrier annihilation effect caused by cut edges. Figure 6 clearly shows that the sample size of $2.3 \times 1.0 \text{ cm}^2$ was not large enough for precise measurement of τ_{eff} free of the edge effect in the cases of high minority carrier effective lifetime and CW light illumination, because minority carriers propagate over a long distance. The results shown in Figs. 3–5 suggest that an additional 0.9 cm surrounding measurement area is necessary. In the case of measurement area of $2.3 \times 1.0 \text{ cm}^2$, the sample size should be larger than $4.2 \times 2.8 \text{ cm}^2$. Even if the measurement area is very small, for example a laser light probe spot for photoluminescence measurement method, the sample size should be larger than the area with a diameter of 1.8 cm.

Figure 7 shows the linear plot of the experimental spatial distribution of τ_{eff} (a) and its logarithmic plot (b) as functions of X_1 from -2.0 to 2.0 cm for the sample with the SiO_2 layers in the right half region (positive X_1) and the bare

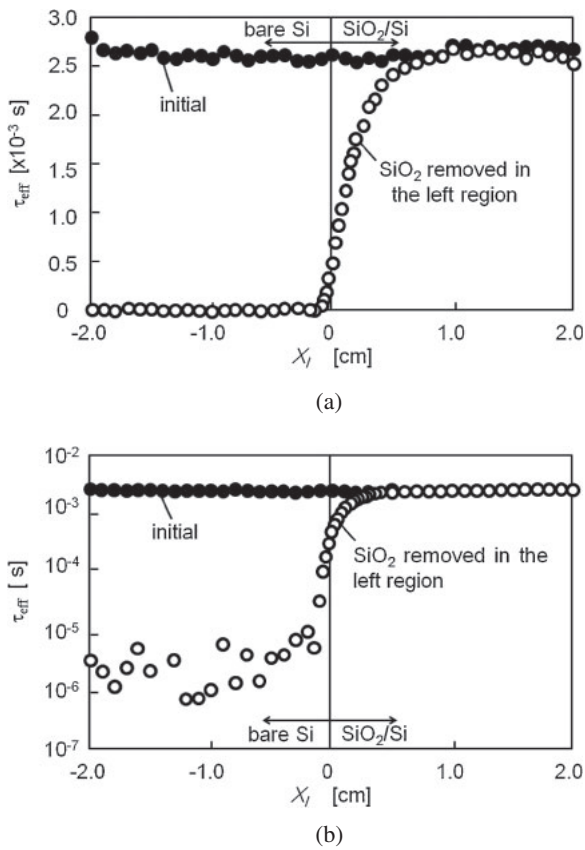


Fig. 7. Linear plots of the experimental spatial distribution of τ_{eff} (a) and their logarithmic plots (b) as functions of X_1 direction from -2.0 to 2.0 cm for the sample with the SiO_2 layers in the right half region (positive X_1) and bare surface in left half region (negative X_1) at both surfaces, as shown in Fig. 1(b).

surface in left half region (negative X_1) at both surfaces, as shown in Fig. 1(b). The spatial distributions of τ_{eff} for the initial sample entirely coated with thermally SiO_2 layers were also plotted in Fig. 7. τ_{eff} had high values in the range from 2.5×10^{-3} to 2.8×10^{-3} s for the initial sample. It was also high from 2.5×10^{-3} to 2.7×10^{-3} s at X_1 higher than 0.9 cm for the sample with remaining SiO_2 layers in the right half. τ_{eff} gradually decreased as the position of light illumination approached to the edges of the bare surface region, as shown in Fig. 7. It decreased to about one-fifth of that of the initial sample, 5.0×10^{-4} s, at X_1 of 0 cm. This means that the minority hole carrier density decreased in the right region at positive X_1 because of diffusion to the lateral direction toward the edge of the bare surface region. The gradual decrease in τ_{eff} over a long distance of 0.9 cm shown in Fig. 7 is a similar behavior to that for the sample with cut edge, as shown in Fig. 3. The results shown in Fig. 7 support that τ_{eff} decreased near the cut edge via simple carrier diffusion to the high-carrier-recombination region. On the other hand, τ_{eff} rapidly decreased in the bare surface region, as shown in Fig. 7(b). τ_{eff} decreased to 1.0×10^{-4} s at -0.08 cm, which was about one fifth of that at 0 cm. It was lower than 7×10^{-6} s between -0.15 and -2.0 cm. These results indicate that hole minority carriers were rapidly annihilated by high densities of surface recombination defect states at the bare surfaces. In that region, carrier diffusion in the depth direction was important and τ_{eff} was

governed by S at both bare surfaces. D was not important because the film thickness, 0.05 cm, was much smaller than the carrier diffusion length in the depth direction, which was 0.17 cm [$\sim(D \cdot \tau_{\text{eff}})^{0.5} = (12 \times 2.5 \times 10^{-3})^{0.5}$]. Our numerical calculation showed that the S values of the bare surfaces were in the range from 4000 to 40000 cm/s (analysis limit). The high S probably resulted from the formation of native oxide at the surface when the samples were kept in air atmosphere. The S of the bare surfaces was much higher than the most possible S_E of 500 cm/s at the cut edges as described above. The cut edge surface was also bare and must have had native oxide layer after cutting. We believe that the big difference between S_E and S resulted from the accuracy measurement of changes in τ_{eff} in the lateral direction over a long distance of up to 0.9 cm. Changes in τ_{eff} over a long distance depends on D . This reduces the accuracy of determining S_E . It will be possible for S_E to be 4000 cm/s or higher, as shown in Fig. 4. The results in Figs. 3–7 show that passivation of the surface including the cut surface are very important for achieving high performance over the whole area for photovoltaic and photosensor devices.

4. Conclusions

We investigated the minority carrier annihilation effect caused by cut edges and partially formed bare surfaces for $500\text{-}\mu\text{m}$ -thick n-type silicon substrates coated with thermally grown SiO_2 layers. Samples were mechanically cut in air atmosphere to form bare silicon surface edges. Samples with partially bare silicon surfaces were also formed by the chemical etching method. In order to precisely measure the spatial distribution of τ_{eff} , we used a 9.35 GHz microwave transmittance measurement system with a 0.2 cm wide light beam for 635 nm light illumination. A decrease in τ_{eff} was observed in the region of 0.9 cm near the cut edges. τ_{eff} markedly decreased from 3.4×10^{-3} (initial) to 6.5×10^{-4} s at the cut edges. This shows that serious recombination defect states are generated at the cut bare surface. A finite differential numerical calculation with a simple carrier diffusion model in the lateral direction with a τ_{eff} of 3.4×10^{-3} s, a diffusion coefficient of 12 cm²/s, and a recombination velocity of 500 cm/s at the cut edges well explained the experimental decrease in τ_{eff} . A silicon piece cut with the same size 2.3×1.0 cm² as the cross section of the waveguide tube showed a decrease in τ_{eff} by 30% compared with 2.5×10^{-3} s of the initial 4-in. samples coated with thermally grown SiO_2 . This suggests that samples larger than the measurement area is necessary for investigation of minority carrier behaviors under CW light illumination. A similar wide-range decrease in τ_{eff} was observed near the bare silicon surface edge formed by partial etching of SiO_2 layers. Bare silicon had a high recombination velocity above 4000 cm/s. The hole minority carriers diffused to the bare silicon from the region coated with SiO_2 layers and its τ_{eff} decreased.

Acknowledgments

This work was partly supported by a Grant-in-Aid for Science Research C (No. 22560292) from the Ministry of Education, Culture, Sports, Science and Technology of Japan, Sameken Corporation, and Designsystem.

- 1) A. Rohatagi: Proc. 3rd World Conf. Photovoltaic Energy Conversion, 2003, A29.
- 2) M. A. Green: *Prog. Photovoltaics* **17** (2009) 183.
- 3) S. M. Sze: *Semiconductor Devices* (Wiley, New York, 1985) Chaps. 6 and 7.
- 4) G. S. Kousik, Z. G. Ling, and P. K. Ajmera: *J. Appl. Phys.* **72** (1992) 141.
- 5) J. M. Borrego, R. J. Gutmann, N. Jensen, and O. Paz: *Solid-State Electron.* **30** (1987) 195.
- 6) G. W. 't Hooft, C. Van Oopdorp, H. Veenvliet, and A. T. Vink: *J. Cryst. Growth* **55** (1981) 173.
- 7) H. Daio and F. Shimura: *Jpn. J. Appl. Phys.* **32** (1993) L1792.
- 8) J. Sritharathikhun, C. Banerjee, M. Otsubo, T. Sugiura, H. Yamamoto, T. Sato, A. Limmanee, A. Yamada, and M. Konagai: *Jpn. J. Appl. Phys.* **46** (2007) 3296.
- 9) Y. Takahashi, J. Nigo, A. Ogane, Y. Uraoka, and T. Fuyuki: *Jpn. J. Appl. Phys.* **47** (2008) 5320.
- 10) M. Boulou and D. Bois: *J. Appl. Phys.* **48** (1977) 4713.
- 11) Y. Ogita: *J. Appl. Phys.* **79** (1996) 6954.
- 12) C. Munakata: *Jpn. J. Appl. Phys.* **43** (2004) L1394.
- 13) T. Sameshima, H. Hayasaka, and T. Haba: *Jpn. J. Appl. Phys.* **48** (2009) 021204.
- 14) T. Sameshima, T. Nagao, S. Yoshidomi, K. Kogure, and M. Hasumi: *Jpn. J. Appl. Phys.* **50** (2011) 03CA02.
- 15) T. Sameshima, R. Ebina, K. Betsuin, Y. Takiguchi, and M. Hasumi: *Jpn. J. Appl. Phys.* **52** (2013) 011801.
- 16) C. C. Chao, R. Chleboski, E. J. Henderson, C. K. Holmes, J. P. Kalejs, and T. S. Gross: *MRS Proc.* **226** (1991) 363.
- 17) F. Z. Fang and V. C. Venkatesh: *CIRP Ann.—Manuf. Technol.* **47** (1998) 45.
- 18) A. M. Emel'yanov: *Phys. Semicond. Devices* **45** (2011) 805.
- 19) F. W. Chen and J. E. Cotter: *Appl. Phys. Lett.* **89** (2006) 263509.
- 20) J. Schmidt and A. G. Aberle: *J. Appl. Phys.* **81** (1997) 6186.
- 21) E. D. Palk: *Handbook of Optical Constants of Solids* (Academic Press, London, 1985) p. 547.
- 22) A. S. Groove: *Physics and Technology of Semiconductor Devices* (Wiley, New York, 1967) Chap. 5.
- 23) J. Furukawa, T. Nagao, and T. Sameshima: Proc. Workshop Active Matrix Flat Panel Displays, 2012, P-44.
- 24) H. Henzler and J. Clabes: *Jpn. J. Appl. Phys.* **13** (1974) Suppl. 2, Pt. 2, p. 389.
- 25) H. Ibach, K. Horn, R. Dorn, and H. Lueth: *Surf. Sci.* **38** (1973) 433.
- 26) Y. Taur and T. Ning: *Fundamental of Modern VLSI Physics* (Cambridge University Press, Cambridge, U.K., 1998) Chap. 2.